

Ruling out color transparency in quasi-elastic $^{12}\text{C}(e,e'p)$ up to Q^2 of 14.2 (GeV/c) 2

D. Bhetuwal,¹ J. Matter,² H. Szumila-Vance,³ M. L. Kabir,¹ D. Dutta,¹ R. Ent,³ D. Abrams,² Z. Ahmed,⁴ B. Aljawrneh,⁵ S. Alsalmi,⁶ R. Ambrose,⁴ D. Androic,⁷ W. Armstrong,⁸ A. Asaturyan,⁹ K. Assumin-Gyimah,¹ C. Ayerbe Gayoso,^{10,1} A. Bandari,¹⁰ S. Basnet,⁴ V. Berdnikov,¹¹ H. Bhatt,¹ D. Biswas,¹² W. U. Boeglin,¹³ P. Bosted,¹⁰ E. Brash,¹⁴ M. H. S. Bukhari,¹⁵ H. Chen,² J. P. Chen,³ M. Chen,² E. M. Christy,¹² S. Covrig,³ K. Craycraft,¹⁶ S. Danagoulian,⁵ D. Day,² M. Diefenthaler,³ M. Dlamini,¹⁷ J. Dunne,¹ B. Duran,⁸ R. Evans,⁴ H. Fenker,³ N. Fomin,¹⁶ E. Fuchey,¹⁸ D. Gaskell,³ T. N. Gautam,¹² F. A. Gonzalez,¹⁹ O. Hansen,³ F. Hauenstein,²⁰ A. V. Hernandez,¹¹ T. Horn,¹¹ G. M. Huber ,⁴ M. K. Jones,³ S. Joosten,⁸ A. Karki,¹ C. Keppel,³ A. Khanal,¹³ P. King,¹⁷ E. Kinney,²¹ H. S. Ko,²² M. Kohl,¹² N. Lashley-Colthirst,¹² S. Li,²³ W. B. Li,¹⁰ A. H. Liyanage,¹² D. Mack,³ S. Malace,³ P. Markowitz,¹³ D. Meekins,³ R. Michaels,³ A. Mkrtchyan,⁹ H. Mkrtchyan,⁹ S. J. Nazeer,¹² S. Nanda,¹ G. Niculescu,²⁴ I. Niculescu,²⁴ D. Nguyen,² Nuruzzaman,²⁵ B. Pandey,¹² S. Park,¹⁹ E. Pooser,³ A. Puckett,¹⁸ M. Rehfuss,⁸ J. Reinhold,¹³ N. Santiesteban,²³ B. Sawatzky,³ G. R. Smith,³ A. Sun,²⁶ V. Tadevosyan,⁹ R. Trotta,¹¹ S. A. Wood,³ C. Yero,¹³ and J. Zhang¹⁹

(for the Hall C Collaboration)

¹Mississippi State University, Mississippi State, Mississippi 39762, USA

²University of Virginia, Charlottesville, Virginia 22903, USA

³Thomas Jefferson National Accelerator Facility, Newport News, Virginia 23606, USA

⁴University of Regina, Regina, Saskatchewan S4S 0A2, Canada

⁵North Carolina A & T State University, Greensboro, North Carolina 27411, USA

⁶Kent State University, Kent, Ohio 44240, USA

⁷University of Zagreb, Zagreb, Croatia

⁸Temple University, Philadelphia, Pennsylvania 19122, USA

⁹A.I. Alikhanyan National Science Laboratory

(Yerevan Physics Institute), Yerevan 0036, Armenia

¹⁰The College of William & Mary, Williamsburg, Virginia 23185, USA

¹¹Catholic University of America, Washington, DC 20064, USA

¹²Hampton University, Hampton, Virginia 23669, USA

¹³Florida International University, University Park, Florida 33199, USA

¹⁴Christopher Newport University, Newport News, Virginia 23606, USA

¹⁵Jazan University, Jazan 45142, Saudi Arabia

¹⁶University of Tennessee, Knoxville, Tennessee 37996, USA

¹⁷Ohio University, Athens, Ohio 45701, USA

¹⁸University of Connecticut, Storrs, Connecticut 06269, USA

¹⁹Stony Brook University, Stony Brook, New York 11794, USA

²⁰Old Dominion University, Norfolk, Virginia 23529, USA

²¹University of Colorado Boulder, Boulder, Colorado 80309, USA

²²Institut de Physique Nucleaire, Orsay, France

²³University of New Hampshire, Durham, New Hampshire 03824, USA

²⁴James Madison University, Harrisonburg, Virginia 22807, USA

²⁵Rutgers University, New Brunswick, New Jersey 08854, USA

²⁶Carnegie Mellon University, Pittsburgh, Pennsylvania 15213, USA

(Dated: October 22, 2020)

Quasielastic $^{12}\text{C}(e,e'p)$ scattering was measured at negative 4-momentum transfer squared $Q^2 = 8, 9.4, 11.4,$ and 14.2 (GeV/c) 2 , the highest ever achieved to date. Nuclear transparency for this reaction was extracted by comparing the measured yield to that expected from a plane-wave impulse approximation calculation without any final state interactions. The measured transparency was consistent with no Q^2 dependence, up to momentum scales where earlier $A(p,2p)$ results had indicated a rise in transparency, ruling out the quantum chromodynamics effect of color transparency at such momentum scales. These results impose strict constraints on models of color transparency for protons.

One of the dominant elements of the nuclear many body problem governing the propagation of hadrons through the nuclear medium is a “reduction of flux”. For example, in the quasielastic scattering of electrons from a nucleus, $A(e,e'p)$, the outgoing proton in the elementary ep elastic scattering can undergo final state interactions (FSI) with the spectator nucleons. These interactions can lead to the absorption and/or rescattering of the outgoing proton resulting in the reduction of the measured $A(e,e'p)$ yield, where the scattered electron and proton are detected in coincidence. This reduction of the coincidence yield can be quantified

in terms of the nuclear transparency (T), defined for the $A(e, e'p)$ process as the ratio of the measured the calculated Plane Wave Impulse Approximation (PWIA) yield. The PWIA yield is calculated in the absence of FSI as well as initial state interactions (ISI). Nuclear transparency for the $A(e, e'p)$ process is then the probability that the knocked-out proton escapes the nucleus without further interactions with the spectator nucleons. Thus, the measurement of T remains of interest for insight into the nuclear many body problem and the strong interaction between hadrons and nuclei [1].

At low energies, the strong interaction is well described in terms of nucleons (protons and neutrons) exchanging mesons [2], whereas at high energies, perturbative Quantum Chromodynamics (pQCD) characterizes the strong force in terms of quarks and gluons carrying color charge. Although these two descriptions are well understood in their respective energy scales, the transition between them is not uniquely identified. Quantum Chromodynamics (QCD) predicts that protons produced in exclusive processes at sufficiently high 4-momentum transfer (Q), will experience suppressed final (initial) state interactions resulting in a significant enhancement in the nuclear transparency [3]. This unique prediction of QCD is named color transparency (CT), and the observation of the onset of CT may help identify the transition between the two alternate descriptions of the strong force. Measurement of T can therefore test for deviation from the expectations of conventional nuclear physics and the onset of quark-gluon degrees of freedom.

Mueller and Brodsky [3] introduced CT as a direct consequence of the concept that in exclusive processes at sufficiently high momentum transfer, hadrons are produced in a small point-like configuration (PLC). Quantum mechanics accounts for the existence of hadrons that fluctuate to a PLC, and a high momentum transfer virtual photon preferentially interacts with a hadron in a PLC (with transverse size $r_{\perp} \approx 1/Q$). This phenomenon is sometimes referred to as “squeezing” [4]. The reduced transverse size, color neutral PLC is screened from external fields, analogous to a reduced transverse size electric dipole [4]. At sufficiently high Lorentz factor, the PLC maintains its compact size long enough (referred to as “freezing”) to traverse the nuclear volume while experiencing reduced interaction with the spectator nucleons. It thereby experiences reduced attenuation in the nucleus due to color screening and the properties of the strong force [4]. The onset of CT is thus a signature of QCD degrees of freedom in nuclei and is expected to manifest as an increase in T with increasing momentum transfer.

CT is well-established at high energies, see for example Ref. [1], but the energy regime for the onset of CT is less well known. In fact, the suppression of further interactions with the nuclear medium is a fundamental

assumption necessary to account for Bjorken scaling in deep-inelastic scattering at small x_B [5]. Moreover, the onset of CT is of specific interest as it can help identify the relevant 4-momentum transferred squared (Q^2) where factorization theorems are applicable [6] enabling the extraction of Generalized Parton Distributions (GPDs) [7, 8]. At intermediate energies, there exists a trade off between the selection of the PLC and its expansion as it transits the nucleus. Therefore, the onset of CT is best observed at the intermediate energy regime where the expansion distance of the PLC becomes significant compared to the nuclear radius. Theory anticipates that it is more probable to observe the onset of CT at lower energies for meson production than for baryons as it is more probable for quark-antiquark pairs (mesons) to form a PLC than three quark systems (baryons) [9]. Additionally, the significantly larger Lorentz factor for mesons ensures that the expansion distance over which the PLC fluctuates back to its equilibrium configuration can be as large as the nuclear radius at lower energies for mesons than for baryons [10].

The predicted onset of CT for final-state mesons has been demonstrated in several experiments at Jefferson Lab (JLab). Pion photoproduction cross sections of ${}^4\text{He}$ to ${}^2\text{H}$ were found to be consistent with CT theories showing a positive rise in the ratio [11]. Precise and systematic studies of pion electroproduction on a range of targets established a positive slope in the transparency ratios for Q^2 in the range from 1–5 (GeV/c) 2 , as well as an A -dependence of the slope. These results were found to be consistent with models that include CT [12, 13]. The onset of CT in mesons was further confirmed by a JLab experiment measuring the nuclear transparency of ρ^0 electroproduction which showed slopes vs Q^2 consistent with the same CT models [14] as the pions. While empirical evidence conclusively confirms the onset of CT in mesons at momentum scales corresponding to $Q^2 \approx 1$ (GeV/c) 2 , the observation of the onset of CT in baryons is somewhat ambiguous.

In a pioneering experiment at the Brookhaven National Lab (BNL), the E850 collaboration attempted to measure the onset of CT using a large-angle proton knockout $A(p, 2p)$ reaction [15]. The nuclear transparency was measured as the ratio of the quasielastic cross section from a nuclear target to that of the free pp cross section. The transparency was measured as a function of an effective beam momentum, P_{eff} , and was shown to have a positive rise, consistent with CT, from $P_{\text{eff}} = 5.9\text{--}9$ GeV/c [15]. However, a subsequent decrease in the transparency was observed between $P_{\text{eff}} = 9.5\text{--}14.4$ GeV/c that was not consistent with CT [16–18]. This enhancement and subsequent fall in the nuclear transparency spans a Q^2 (Mandelstam $-t$) range of 4.8–12.7 (GeV/c) 2 and outgoing proton momentum range of 3.3–7.7 GeV/c. Two possible explanations for the decrease in transparency at the higher momenta are: an

179 in-medium suppression of the energy dependence of the pp elastic cross section known as nuclear filtering [19] [20],²³⁷
 180 or the excitation of charmed quark resonances or other²³⁸
 181 exotic multi-quark states [21].²³⁹

183 In the $A(p, 2p)$ reaction both the incoming and out-²⁴¹
 184 going protons experience a reduction of flux making it²⁴²
 185 more challenging to interpret. Consequently, the am-²⁴³
 186 biguous results from the BNL experiment were investi-²⁴⁴
 187 gated with the $(e, e'p)$ process, which employs electrons,²⁴⁵
 188 a weakly interacting probe, to avoid the complication of²⁴⁶
 189 the reduction of flux of the hadronic probe. Furthermore,²⁴⁷
 190 compared to the $(p, 2p)$ process, the elementary elastic ep ²⁴⁸
 191 scattering cross section is accurately known and smoothly²⁴⁹
 192 varying with energy transfer, and the $A(e, e'p)$ process is²⁵⁰
 193 less sensitive to the poorly known large momentum com-²⁵¹
 194 ponents of the nuclear wave function [22].²⁵²

195 Previous $A(e, e'p)$ experiments [23–26] have measured²⁵³
 196 the nuclear transparency of protons on a variety of nuclei²⁵⁴
 197 up to $Q^2 = 8.1$ (GeV/c)². These experiments yielded²⁵⁵
 198 missing energy and momentum distributions consistent²⁵⁶
 199 with conventional nuclear physics and did not observe²⁵⁷
 200 any Q^2 dependence in the nuclear transparency. This²⁵⁸
 201 ruled out the onset of CT for protons at Q^2 values corre-
 202 sponding to outgoing proton momenta of 5 GeV/c, which
 203 in some interpretations is just before the rise of trans-
 204 parency noted in the $A(p, 2p)$ data.

205 The recent 12 GeV upgrade at JLab allows access to
 206 the entire Q^2 range and outgoing proton momentum
 207 range of the BNL experiment for the first time. It
 208 also allows significant overlap between the knocked
 209 out proton momentum in electron scattering and the
 210 effective proton momentum quoted by the BNL $A(p, 2p)$
 211 experiment, within the range where the enhancement in
 212 nuclear transparency was observed [15]. These features
 213 make it possible to explore all possible variables (Q^2 ,
 214 incident or outgoing proton momentum) that could be,
 215 driving the enhancement in transparency observed in the
 216 BNL experiment. In this letter, we report on the latest²⁶⁰
 217 quasi-elastic electron scattering experiment to search for²⁶²
 218 the onset of CT at the upgraded JLab. This experiment²⁶³
 219 extends the nuclear transparency measurements in²⁶⁴
 220 $^{12}\text{C}(e, e'p)$ to the highest Q^2 to date and covers the²⁶⁵
 221 complete kinematic phase space of the enhancement²⁶⁶
 222 observed by the BNL experiment.²⁶⁷

223
 224 The experiment was carried out in Hall C at JLab²⁶⁹
 225 and was the first experiment to be completed in Hall C²⁷⁰
 226 after the upgrade of the continuous wave (CW) electron²⁷¹
 227 beam facility (CEBAF) accelerator. The experiment²⁷²
 228 used the CW electron beam with beam energies of 6.4²⁷³
 229 and 10.6 GeV and beam currents up to 65 μA . The²⁷⁴
 230 total accumulated beam charge was determined with²⁷⁵
 231 $< 1\%$ uncertainty by a set of resonant-cavity based²⁷⁶
 232 beam-current monitors and a parametric transformer²⁷⁷
 233 monitor. The beam energy was determined with an²⁷⁸
 234 uncertainty of 0.1% by measuring the bend angle of²⁷⁹
 235 the beam, on its way into Hall C, as it traversed a²⁸⁰

set of magnets with precisely known field integrals.
 The main production target was a carbon foil of 4.9%
 radiation lengths (rl), while a second carbon foil of 1.5%
 rl was used for systematic studies. The thickness of the
 foils was measured to better than 0.5%. A 10-cm-long
 (726 mg/cm²) liquid hydrogen target was used for
 normalization to the elementary ep scattering process.
 Two aluminum foils placed 10-cm apart were used to
 monitor the background from the aluminum end caps
 of the hydrogen target cell. The beam incident on the
 liquid hydrogen target was rastered over a 2×2 mm²
 area to suppress density variations from localized boiling.

The scattered electrons were detected in the existing
 High Momentum Spectrometer (HMS, momentum accep-
 tance $\Delta p/p \pm 10\%$, solid angle $\Omega = 7$ msr) [25] in co-
 incidence with the knocked-out protons detected in the
 new Super High Momentum Spectrometer (SHMS, mo-
 mentum acceptance $\Delta p/p$ from -10 to +12%, solid angle
 $\Omega = 4$ msr) [27]. The SHMS central angle was chosen to
 detect protons along the electron three-momentum trans-
 fer, \vec{q} . The kinematics of the four different Q^2 settings
 are shown in Table I. The solid angle of the spectrome-

TABLE I. The kinematic settings of the experiment. The
 electron beam energy was 6.4 GeV for the $Q^2 = 8.0$ (GeV/c)²
 setting and 10.6 GeV for the rest. The protons were detected
 along the electron three-momentum transfer, \vec{q} .

Q^2 (GeV/c) ²	θ_e^{lab} (deg)	$p_{e'}$ (GeV/c)	θ_p^{lab} (deg)	p_p (GeV/c)
8.0	45.1	2.125	17.1	5.030
9.4	23.2	5.481	21.6	5.830
11.4	28.5	4.451	17.8	6.882
14.2	39.3	2.970	12.8	8.352

ters was defined for electrons and the coincident $(e, e'p)$
 process by a 2-in-thick tungsten alloy collimator. The
 detector packages in the two spectrometers were similar,
 they included four planes of segmented scintillators
 (except for the last plane in SHMS which used quartz
 bars) that were used to form the trigger and to provide
 time-of-flight information. Two 6-plane drift chambers
 were used to measure particle tracks with better than
 250 μm resolution. The tracking efficiency was contin-
 uously monitored with an uncertainty of $\approx 0.1\%$ for the
 HMS and $< 0.5\%$ for the SHMS. The uncertainty was
 obtained from the average variation of the tracking effi-
 ciency when using three independent criteria for deter-
 mining the efficiency. The typical resolutions in the HMS
 (SHMS) were 0.2% (0.1%) for momentum, 0.8 (0.9) mrad
 for horizontal angle and 1.2 (1.1) mrad for the vertical an-
 gle. In the HMS, a threshold gas Cherenkov detector and
 a segmented Pb-glass calorimeter were used for electron
 identification. The protons in the SHMS were identified
 by coincidence time after excluding pions using a noble-

281 gas threshold Cherenkov detector and a segmented Pb-
 282 glass calorimeter. The pion-to-electron ratio in the HMS
 283 ranged from $\approx 10^{-1}$ to 10^{-3} , while the pion-to-proton
 284 ratio in the SHMS was always < 0.2 . The corrections
 285 for particle energy loss through the spectrometers were
 286 determined to better than 1%. The electron-proton
 287 coincidence events were recorded in 1-hour-long runs via
 288 a pipelined data acquisition system operated using the
 289 CEBAF Online Data Acquisition (CODA) software pack-
 290 age [28]. Singles (inclusive) electron and proton events
 291 were separately recorded for systematic studies.

292 The individual electron and proton tracks for each
 293 coincidence event were reconstructed back to the target.
 294 The coincidence time was determined as the difference
 295 in the time of flight between the two spectrometers with
 296 corrections to account for path-length variations from
 297 the central trajectory and the individual start-times.
 298 The coincidence time spectrum had a width of 380 ps,
 299 sufficiently smaller than the 4 ns beam structure. The
 300 rate of accidental coincidences was $< 0.2\%$.

301
 302 At each kinematic setting, the charge-normalized ex-340
 303 perimental yield for ep coincidences measured on the hy-341
 304 drogen target was compared to a parameterization of the342
 305 known ep elastic scattering cross section [29] through343
 306 a Monte Carlo simulation of the experiment [30] (see344
 307 Fig. 1). The simulation included a realistic model of the345
 308 spectrometer magnetic transport properties, the detailed346
 309 geometries of all the detectors and intervening materials,347
 310 and models for processes such as multiple scattering, ion-348
 311 ization energy loss and radiative effects. The experimen-349
 312 tal yield was corrected for detector and tracking ineffi-350
 313 ciencies, computer and electronic dead-times and proton351
 314 absorption in SHMS. The density of the liquid hydro-352
 315 gen target varies with the incident electron beam current353
 316 (beam boiling effect), and the experimental yield was cor-354
 317 rected for this effect. The correction was determined to355
 318 be $(2.6 \pm 0.4)\%$ at the highest beam current ($65 \mu\text{A}$). The356
 319 hydrogen yield was found to be consistent with the known357
 320 ep elastic scattering world data, validating the analysis358
 321 procedure. The comparison to the Monte Carlo yield359
 322 was used to determine the normalization uncertainty of360
 323 $\pm 1.8\%$. 361

324
 325
 326 The electron beam energy/momentum (E_e/\vec{p}_e)363
 327 and the energy/momentum of the scattered electron364
 328 ($E_{e'}/\vec{p}_{e'}$) measured by the HMS were used to determine365
 329 $\vec{q} = \vec{p}_e - \vec{p}_{e'}$ and the energy transfer $\nu = E_e - E_{e'}$ 366
 330 for each coincidence event. The kinetic energy ($T_{p'}$)367
 331 and momentum ($\vec{p}_{p'}$) of knocked out protons measured368
 332 in the SHMS were used to determine the missing369
 333 energy $E_m = \nu - T_{p'} - T_{A-1}$ and missing momentum370
 334 $\vec{p}_m = \vec{p}_{p'} - \vec{q}$ for the coincidence event, where T_{A-1} is371
 335 the reconstructed kinetic energy of the $A - 1$ recoiling372
 336 nucleus. The experimental yield on the ^{12}C target was
 337 obtained by integrating the charge-normalized coinci-
 338 dence events over a phase space defined by $E_m < 80$

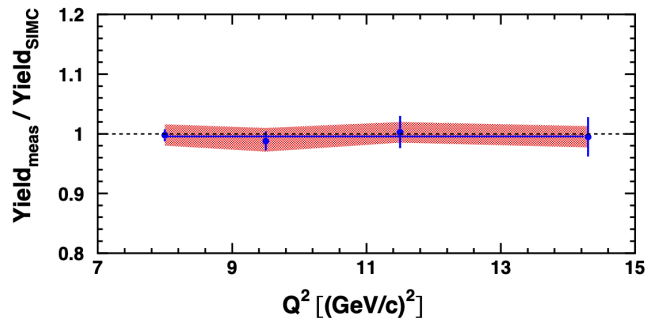


FIG. 1. The ratio of measured yield to the simulation (SIMC) [30] yield is shown for elastic ep scattering from hydrogen for $E_m < 65$ MeV and $|p_m| < 65$ MeV/c. Only the statistical uncertainties are shown. The solid horizontal line is a fit to a constant value with the shaded band representing the normalization uncertainty of 1.8% determined from these yield ratios and includes the $\approx 1\%$ variation in the ratio when the E_m and $|p_m|$ cuts are varied.

MeV and $|\vec{p}_m| < 300$ MeV/c. These constraints eliminate inelastic contributions such as from pion production and ensure exclusivity. The experimental yield was corrected for all known inefficiencies of both spectrometers such as the detector efficiencies (97%-99%), trigger efficiency (98%-99%), tracking efficiencies (99%-HMS and 94%-99%-SHMS), computer and electronic live-times (94%-99%), and proton absorption in the SHMS ($\approx 8\%$). The systematic uncertainty arising from the cut dependence of the experimental yield was determined by varying the cuts one at a time and recording the variation in yields for the different kinematic settings. The quadrature sum of the variation over all the different cuts was used as the event selection uncertainty ($\approx 1.4\%$). The uncertainty due to the livetime and the detector and trigger efficiencies was determined from a set of luminosity scans in each spectrometer performed immediately before and after the experiment on a ^{12}C target. The charge-normalized yield from these scans for each spectrometer was found to be independent of the beam current within statistical uncertainties, and the average variation in the normalized yield vs beam current was recorded as the systematic uncertainty (0.5%). The uncertainty due to the charge measurement was estimated to be $< 1\%$ which was validated by the change in the charge-normalized experimental yield when varying the minimum beam current cut.

A Monte Carlo simulation of the $A(e, e'p)$ process was performed assuming the plane-wave impulse approximation (PWIA) to be valid, in which case the \vec{p}_m is equal to the initial momentum of the proton in the carbon nucleus, and the cross section is calculated in a factorized form as:

$$\frac{d^6\sigma}{dE_{e'}d\Omega_{e'}dE_{p'}d\Omega_{p'}} = E_{p'}|p_{p'}|\sigma_{ep}S(E_m, \vec{p}_m), \quad (1)$$

where $\Omega_{e'}$, $\Omega_{p'}$ are the solid angles of the outgoing electron and proton respectively, σ_{ep} is the off-shell ep cross section and $S(E_m, \vec{p}_m)$ is the spectral function defined as the joint probability of finding a proton with momentum p_m and separation energy E_m within the nucleus. The simulation used the De Forest σ_{1}^{fc} prescription [31] for the off-shell cross section, and the simulated yield was insensitive ($< 0.1\%$) to the off-shell effect. The independent particle spectral functions used in the simulation were the same as the ones used in Ref. [23–26]. The effect of nucleon-nucleon correlations, which cause the single particle strength to appear at high E_m , was included by applying a correction factor of 1.11 ± 0.03 as previously determined in Ref. [32]. The simulated yield was obtained by integrating over the same phase-space volume as for the experimental data. The total model-dependent uncertainty due to the uncertainty in the spectral function (2.8%) and the corrections due to nucleon-nucleon correlations was estimated to be 3.9%.

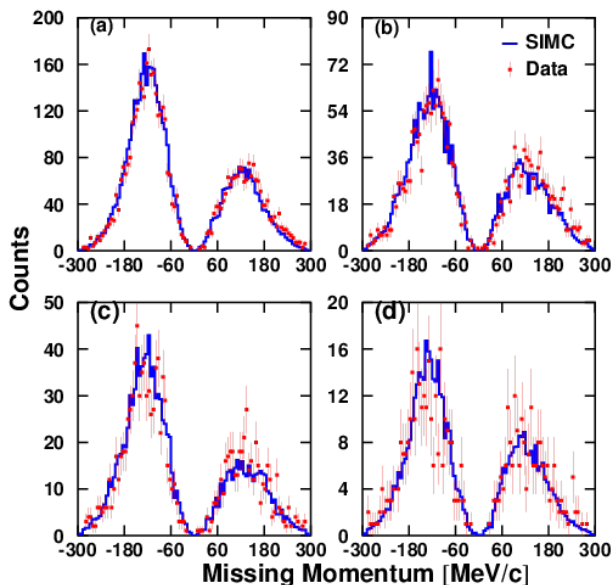


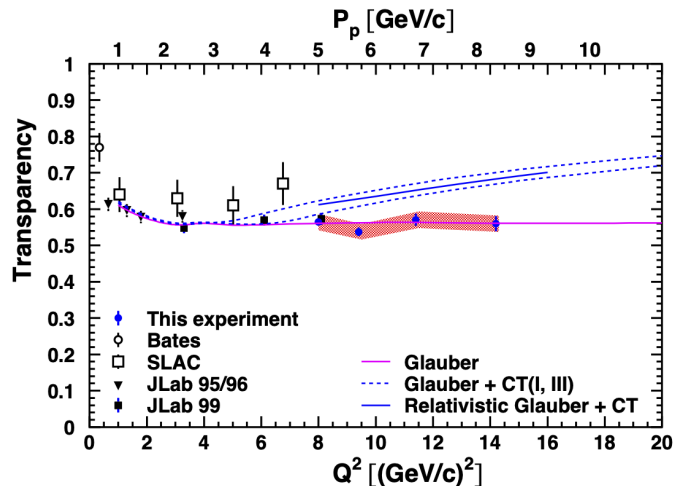
FIG. 2. The missing momentum, p_m , for the carbon data is shown for each kinematic setting. (a) $Q^2 = 8.0$ (b) $Q^2 = 9.4$ (c) $Q^2 = 11.4$ and (d) $Q^2 = 14.2$ (GeV/c)²

The $^{12}\text{C}(e, e'p)$ yields as a function of p_m are shown in Fig 2, along with the simulated yields. The constraint of $E_m < 80$ MeV was applied to both data and simulation. The shape of the data and simulated distributions agree with each other very well for all four Q^2 settings, validating the use of the impulse approximation. It also indicates the robustness of the spectrometer models in the Monte Carlo simulation. The uncertainty from the spectrometer acceptance was estimated to be 2.6% by comparing the measured and simulated focal plane positions and angles as well as the reconstructed angles and momenta at the reaction vertex. The p_m distributions shown in Fig. 2 are very sensitive to the reconstructed

TABLE II. Systematic Uncertainties

Source	Q^2 dependent uncertainty (%)
Spectrometer acceptance	2.6
Event selection	1.4
Tracking efficiency	0.5
Radiative corrections	1.0
Live time & Det. efficiency	0.5
Source	Normalization uncertainty (%)
Free cross section	1.8
Target thickness	0.5
Beam charge	1.0
Proton absorption	1.2
Total	4.0

momenta and angles and the average bin-by-bin difference between the data and simulated spectra normalized to each other was used as the systematic uncertainty due to acceptance. Table II lists the major sources of systematic uncertainty. The total uncertainty is calculated as the quadrature sum. The model dependent uncertainty is not included in the table.



The carbon nuclear transparency from this experiment along with all previous experiments [23–26, 33]. The negative 4-momentum transfer squared is shown along the x -axis (bottom scale), and the momentum of the knocked out proton is also shown along the top scale of the x -axis. The solid magenta line is a Glauber calculation that excludes color transparency effects [34]. The dashed lines are theory predictions including CT [35] for two different set of parameters and the solid blue line is a prediction from a relativistic Glauber calculation with CT [36]. The error bars show the statistical uncertainty while the band shows the 4.0 % systematic uncertainty. The 3.9% model dependent uncertainty is not shown.

The nuclear transparency was extracted as the ratio of experimental yield to the PWIA yield integrated over

the same phase space volume V :

$$T(Q^2) = \frac{\int_V d^3p_m dE_m Y_{exp}(E_m, \vec{p}_m)}{\int_V d^3p_m dE_m Y_{PWIA}(E_m, \vec{p}_m)}, \quad (2)$$

where V is the phase space volume as defined earlier, $Y_{exp}(E_m, \vec{p}_m)$ is the experimental yield and $Y_{PWIA}(E_m, \vec{p}_m)$ is the PWIA yield. The extracted nuclear transparency as a function of Q^2 is shown in Fig. 3 along with all previous measurements. The measured nuclear transparency of carbon is found to be both energy and Q^2 independent up to $Q^2 = 14.2 (\text{GeV}/c)^2$, the highest accessed in quasi-elastic electron scattering to date. The combined data set from all measurements above $Q^2 = 3.0 (\text{GeV}/c)^2$ was fit to a constant value with a reduced χ^2 of 1.3. The outgoing proton momentum of this experiment overlaps with the effective proton momentum of the BNL experiments that reported an enhancement in nuclear transparency [18]. Moreover, the Q^2 and outgoing proton momentum of this experiment is significantly higher than the BNL experiment. Hence, these results rule out CT as a possible cause of the rise in transparency observed by the BNL experiment. The differences governing the observed onset of CT for mesons at Q^2 of about $1 (\text{GeV}/c)^2$ and the absence of onset of CT for protons at more than an order-of-magnitude higher Q^2 may provide strong clues regarding the differences

between two- and three-quark systems. Future experiments at JLab and elsewhere will further quantify such differences for pions, ρ -mesons and photons [37–39].

In summary, exclusive measurements were performed for Q^2 from 8–14.2 $(\text{GeV}/c)^2$ on hydrogen and carbon targets. The nuclear transparency extracted from these measurements is consistent with traditional nuclear physics calculation and do not support the onset of color transparency. The momentum scales accessed in this experiment rule out color transparency as the reason for a rise in transparency noted in $A(p, 2p)$ data. The present results probe down to a transverse-size as small as ≈ 0.05 fm in the three-quark nucleon system, placing very strict constraints on the onset of color transparency at intermediate energies and all current models.

This work was funded in part by the U.S. Department of Energy, including contract AC05-06OR23177 under which Jefferson Science Associates, LLC operates Thomas Jefferson National Accelerator Facility, and by the U.S. National Science Foundation and the Natural Sciences and Engineering Research Council of Canada. We wish to thank the staff of Jefferson Lab for their vital support throughout the experiment. We are also grateful to all granting agencies providing funding support to authors throughout this project.

-
- [1] D. Dutta, K. Hafidi, and M. Strikman. Color transparency: past, present and future. *Progress in Particle and Nuclear Physics*, 69:10, 2012.
- [2] J. Carlson et al. *Rev. of Mod. Phys.*, 87:1067, 2015.
- [3] A. H. Mueller. Proceedings of the Seventeenth Recontres de Moriond Conference on Elementary Particle Physics. Les Arcs, France, 1983.
- [4] S. J. Brodsky, L. Frankfurt, J. F. Gunion, A. H. Mueller, and M. Strikman. *Phys. Rev. D*, 50:3134, 1994.
- [5] L. Frankfurt and M. Strikman. *Phys. Rep.*, 160:235, 1988.
- [6] M. Strikman. *Nucl. Phys. A*, 663-664:64c–73c, 2000.
- [7] X. Ji. *Phys. Rev. Lett.*, 78:610, 1997.
- [8] A. V. Radyushkin. *Phys. Rev. D*, 56:5524–5557, Nov 1997.
- [9] M. Eides, L. Frankfurt, and M. Strikman. *Phys. Rev. D*, 59:114025, 1999.
- [10] M. Vanderhaeghen, P. A. M. Guichon, and M. Guidal. *Phys. Rev. D*, 60:094017, 1999.
- [11] D. Dutta et al. *Phys. Rev. C*, 68:021001R, 2003.
- [12] B. Clasie et al. *Phys. Rev. Lett.*, 99:242502, 2007.
- [13] X. Qian et al. *Phys. Rev. C*, 81:055209, 2010.
- [14] L. El-Fassi et al. *Phys. Lett. B*, 712:326, 2012.
- [15] A. S. Carroll et al. *Phys. Rev. Lett.*, 61:1698, 1988.
- [16] I. Mardor et al. *Phys. Rev. Lett.*, 81:5085, 1998.
- [17] A. Leksanov et al. *Phys. Rev. Lett.*, 87:212301, 2001.
- [18] J. Aclander et al. *Phys. Rev. C*, 70:015208, Jul 2004.
- [19] J. P. Ralston and B. Pire. *Phys. Rev. Lett.*, 61:1823, 1990.
- [20] B. Kundu, J. Samuelsson, P. Jain, and J. P. Ralston. *Phys. Rev. D*, 62:113009, 2000.
- [21] S. J. Brodsky and G. F. de Teramond. *Phys. Rev. Lett.*, 60:1924, 1988.
- [22] G. R. Farrar, H. Liu, L. L. Frankfurt, and M. I. Strikman. *Phys. Rev. Lett.*, 62:1095, 1989.
- [23] N. C. R. Makins et al. *Phys. Rev. Lett.*, 72:1986, 1994.
- [24] T. G. O’Neill et al. *Phys. Lett.*, 351:87, 1995.
- [25] D. Abbott et al. *Phys. Rev. Lett.*, 80:5072, 1998.
- [26] K. Garrow et al. *Phys. Rev. C*, 66:044613, 2002.
- [27] The SHMS spectrometer in Hall-C. *publication in preparation*.
- [28] <https://coda.jlab.org/drupal/>.
- [29] P. Bosted. *Phys. Rev. C*, 51:409, 1995.
- [30] <https://hallcweb.jlab.org/simc/>.
- [31] T. De Forest. *Nucl. Phys. A*, 392(2):232 – 248, 1983.
- [32] T. G. O’Neill. PhD thesis, California Institute of Technology (unpublished), 1994.
- [33] G. Garino et al. *Phys. Rev. C*, 45:780, 1992.
- [34] V. R. Pandharipande and S. C. Pieper. *Phys. Rev. C*, 45:791, 1992.
- [35] L. L. Frankfurt et al. *Phys. Rev. C*, 51:3435, 1995.
- [36] W. Cosyn, M. C. Martinez, J. Ryckebusch, and B. Van Overmeire. *Phys. Rev. C*, 74:062201(R), 2006.
- [37] D. Dutta, R. Ent, et al. Proposal for JLab experiment E12-06-107.
- [38] K. Hafidi, B. Mustapa, M. Holtrop, et al. Proposal for JLab experiment E12-07-103.
- [39] A. Somov, O. Hen, et al. Proposal for JLab experiment PR12-17-007.